John G. Michopoulos[1]
Fellow ASME
Computational Multiphysics Systems Laboratory,
Center of Materials Physics and Technology,
U.S. Naval Research Laboratory,
Washington, DC 20375
e-mail: john.michopoulos@nrl.navy.mil

Athanasios P. Iliopoulos
Mem. ASME
Computational Multiphysics Systems Laboratory,
Center of Materials Physics and Technology,
U.S. Naval Research Laboratory,
Washington, DC 20375
e-mail: athanasios.iliopoulos@nrl.navy.mil

Nicole A. Apetre
Computational Multiphysics Systems Laboratory,
Center of Materials Physics and Technology,
U.S. Naval Research Laboratory,
Washington, DC 20375
e-mail: nicole.apetre@nrl.navy.mil

John C. Steuben
Mem. ASME
Computational Multiphysics Systems Laboratory,
Center of Materials Physics and Technology,
U.S. Naval Research Laboratory,
Washington, DC 20375
e-mail: john.steuben@nrl.navy.mil

Andrew J. Birnbaum
Computational Multiphysics Systems Laboratory,
Center of Materials Physics and Technology,
U.S. Naval Research Laboratory,
Washington, DC 20375
e-mail: andrew.birnbaum@nrl.navy.mil

Evolution of Sliding Contact Wear Between Deformable Conducting Bodies via a Multiphysics Framework

A multiphysics computational framework is introduced and exercised to predict the wear behavior of two deformable, heat-conducting bodies under conditions of sliding contact. This framework enables the solution of a coupled system of partial differential equations (PDEs) expressing the conservation of energy and momentum along with two ordinary differential equations (ODEs) expressing mass conservation. This system is intended to capture wear evolution for each of the bodies forming a wear pair, in a self-consistent manner. Furthermore, an arbitrary-Lagrangian-Eulerian approach has been integrated to enable tracking the evolution of the wear fronts on both elements of the sliding contact pair through physics-informed mesh deformation. A theorem and a corollary are proved to indicate that most existing models describing wear that are expressed in the form of an ODE are actually manifestations of the law of conservation of mass. The framework is applied for two distinct slider-base pairs. The first involves an aluminum alloy slider and a copper alloy base. The second pair is identical to the first except it contains a thin strip of soda-lime glass embedded in the surface of the base. The effects of this glass layer on the wear of all participating bodies in comparison to the pair that does not contain this layer are presented. They indicate that while the glass layer has a wear mitigation effect for the stationary base it slightly increases the wear of the slider when compared with the respective bodies when the glass is not present.
[DOI: 10.1115/1.4047075]

Keywords: multiphysics modeling and simulation, physics-based simulations, wear, conservation laws, coupled multiphysics

Introduction

The prediction of wear evolution for slider pairs under various regimes of relative velocity, pressure, and temperature has long been a topic of intense interest motivated by the need for design, lifetime estimation, and performance qualification capabilities. Examples of mutliphysics problems involving wear applications are found in bio-tribology for prosthetic limbs and implants, power generation and consumption rotating machinery, electrical third rail contact interface of railway transportation systems, the slider-rail pairs for rocket launching applications, and the armature-rail interfaces of electromagnetic launch systems.

Various attempts have been made [1–8] to model and simulate the evolution of wear via the use of numerical techniques such as finite element analysis (FEA). However, the vast majority of all these efforts focus on addressing the wear of only one of the two interacting bodies and address only a limited amount of physics via partial adherence to the conservation laws. Another limitation observed in these studies is the fact that they address simple geometries such as that of the pin on a disk, inspired by the corresponding well-known tribological characterization device, and lack the flexibility to address arbitrary pair shape arrangements.

The present work describes a computational framework aiming to address these issues, under a top–down self-consistent (i.e., not ignoring any conservation law) multiphysics approach for the general case of interacting deformable heat-conducting wearing bodies.

Furthermore, in the last 6 years, it has been demonstrated that for both cases of stationary [9–11] and sliding contact [12] under multiphysics conditions, top-down fully coupled approaches that solve the PDEs expressing the relevant conservation laws are not only extremely computationally costly for realistically sized problems, but they become even more expensive when wear mechanisms are accounted for. In the past 2 years, our group has embarked on an effort to address this problem by introducing and exercising the proposed computational framework for predicting the wear of two bodies across a sliding contact. Preliminary results of this work has been presented on the 2018 and 2020 ASME IDETC/CIE conferences [13,14]. The present work combines and generalizes these earlier efforts.

The efficiency of the proposed methodology is based on the consideration that, in addition to energy and momentum conservation, the wear behavior of tribological components is encapsulated by one-dimensional, time-dependent rate equations instead of the full mass conservation PDEs governing mass loss due to the various mechanisms present at the interface. In this approach, two general ordinary differential equations (ODEs) are introduced to describe the evolution of wear of the sliding pair components at every point on the interface, coupled directly through the state variables of interest as they are determined by solving the PDEs describing

[1]Corresponding author.

Manuscript received October 22, 2019; final manuscript received April 24, 2020; published online May 26, 2020. Assoc. Editor: Yan Wang.

the macroscopic behavior of the system. This approach exploits the idea that wear depends only on the involved state variables in a point-wise manner without neighboring area dependence. The source terms of the ODEs expressing wear evolution are used to adjust the participating interface physics. The employment of any low-dimensional wear model (i.e, mechanical failure, phase transformation-based, etc.) in a computationally detailed and efficient manner constitutes the main advantage of the approach.

The authors could not identify the existence of any experimental data for the simultaneous wear of both members of any tribo-pair, and therefore, the validation of the multiphysics formalism introduced and implemented in the proposed framework was deemed outside the context of the present work. Nevertheless, in addition to the description of the theoretical foundations of the framework, a verification of its functionality will also be presented by application to two different sliding pairs. The first will involve a pair of dissimilar metal alloys; the second will involve the same pair of dissimilar alloys with the addition of a glass coating covering part of the contact surface of the static member of the tribo-pair. This selection was motivated by the need to explore the potential benefits of glassy coatings to mitigate wear for high-speed sliding contact applications [15] in the area of electromagnetic launch technologies. A number of earlier efforts utilizing glass coatings have been made since the 1950s [16] through the 1970s [17–19]. The technology utilized for applying glass coatings utilizes the Ugine–Sejournet process [20] and was developed for facilitating the extrusion of metallic materials. The motivation for this wear mitigation approach has long been based on the idea that it exploits both the low friction of the liquid glass phase and the thermally insulative properties of the respective glass coatings.

The present paper continues with an overview of the theoretical background of the proposed framework. A description of its computational implementation follows in the "Theoretical Framework for Modeling the Evolution of Sliding Contact" section. Exercising the framework for two tribo-pairs where one contains glass coating is presented in the subsequent section. The final section contains conclusions and plans for the future.

Theoretical Framework for Modeling the Evolution of Sliding Contact

Conservation Laws. The multiphysics framework first introduced in Ref. [13] is based on the conservation laws applicable for the case of deformable and conductive bodies participating in a sliding contact. The idealization of a tribological pair (or "tribo-pair") is presented in Fig. 1, and it consists of the deformable and heat-conducting stationary base and the moving slider.

The wear induced mass loss of both bodies because of their mutual interaction suggests that the thermodynamics to be considered here should involve the presence of open systems in order to allow mass fluxes across the boundaries. The general form of any conservation law for a quantity Φ per unit volume conserved in a body of volume V bounded by surface S can be expressed as

$$\frac{d}{dt}\int_V \Phi dV = -\int_S \boldsymbol{F}\cdot d\boldsymbol{S} - \int_S \Phi \boldsymbol{v}\cdot d\boldsymbol{S} + \int_V R dV \tag{1}$$

where $\boldsymbol{F}$ is flux of the quantity Φ through the boundary S, $\boldsymbol{v}$ is the transport velocity of Φ through the boundary S, R is the source or sink of Φ, and $d\mathbf{S}$ is the vector normal on a small patch of the surface S. This relation essentially indicates that the change of the volume integral of Φ per unit time, as it is shown on the left–hand side, is equal to the sum of the amount of its flux $\boldsymbol{F}$ entering the surface of the body, its convective transport through the surface of the body and the source generated in the volume of the body as they are depicted by the three terms of the right–hand side.

Application of the Gauss–Ostrogradsky divergence theorem on Eq. (1) allows the conversion of the surface integrals to volume integrals and yields the expression

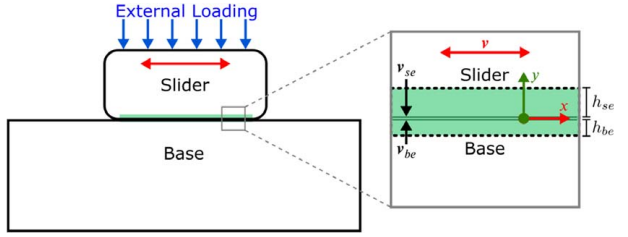

Fig. 1 Example of a tribological pair (left) along with a magnification of the control volume around the interface (right)

$$\frac{d}{dt}\int_V \Phi dV = -\int_V \nabla\cdot\boldsymbol{F} dV - \int_V \nabla\cdot(\Phi\boldsymbol{v}) dV + \int_V R dV \tag{2}$$

Because in an inertial frame the surface and volume are fixed, the time derivative of the summed properties is equal to the sum of the local time derivatives or alternatively,

$$\frac{d}{dt}\int_V \Phi dV = \int_V \frac{\partial\Phi}{\partial t} dV \tag{3}$$

Combining the last two equations leads to the following form of Eq. (2)

$$\int_V \left[\frac{\partial\Phi}{\partial t} + \nabla\cdot(\boldsymbol{F} + \Phi\boldsymbol{v}) - R\right] dV = 0 \tag{4}$$

Since V is of arbitrary shape and size, Eq. (4) can only be satisfied if the sum of terms in square brackets is zero everywhere (or at least for every random volume element). Therefore, the local form of the generalized conservation law can be written as

$$\frac{\partial\Phi}{\partial t} + \nabla\cdot(\boldsymbol{F} + \Phi\boldsymbol{v}) - R = 0 \tag{5}$$

The conservation of mass, momentum, and energy can now be expressed by substituting the proper quantities displayed in Table 1 into Eqs. (1)–(5). These substitutions in Eq. (5) produce the system of the three coupled PDEs expressing, respectively, the conservation of mass, momentum, and energy, to be solved as described subsequently in the present work. In fact, these substitutions in Eq. (5) produce the system of the three coupled PDEs expressing, respectively, the conservation of mass, momentum a, nd energy, to be solved as described subsequently in the present work. In Table 1, the symbols ρ, $\boldsymbol{v}$, $\boldsymbol{t}$, $\boldsymbol{f}$, c_p, T, $\boldsymbol{q}$, and Q represent the mass density, velocity of the deforming medium, the force flux per unit area on the boundary, the body force density, the heat capacity of the medium, the temperature, the heat flux through the boundary, and the heat source density per unit of volume of the material, respectively.

Assuming that the material system is closed (i.e., no loss of mass via the boundaries) and that the particle velocities of the deformable bodies due to the deformation response of the system are small and introducing the expressions defined in Table 1 into the Eq. (5) yields the specific local forms of the conservation laws as follows:

$$\frac{\partial\rho}{\partial t} + \nabla\cdot(\rho\boldsymbol{v}) = 0 \tag{6a}$$

Table 1 Conservation law specialization

	Φ	$\boldsymbol{F}$	R
Mass	ρ	0	0
Momentum	$\rho\boldsymbol{v}$	$\boldsymbol{t}$	$\boldsymbol{f}$
Energy	$\rho c_p T$	$\boldsymbol{q}$	Q

$$\frac{\partial(\rho \boldsymbol{v})}{\partial t} + \nabla \cdot \boldsymbol{\sigma} - \boldsymbol{f} = 0 \tag{6b}$$

$$\frac{\partial(\rho C_p T)}{\partial t} + \nabla \cdot \boldsymbol{q} - Q = 0 \tag{6c}$$

In Eq. (6b), the replacement $\boldsymbol{t} = \boldsymbol{n} \cdot \boldsymbol{\sigma}$ has been utilized, where $\boldsymbol{n}$ and $\boldsymbol{\sigma}$ represent the vector normal to the boundary and Cauchy's second-order stress tensor, respectively.

Reduced Complexity of Mass Conservation Law. Figure 1 depicts the material system of interest as a tribological or wear pair consisting of two deformable heat conductors that have the potential to wear on the common interface. As such, each of the participating bodies needs to satisfy Eq. (6) separately and together. This, in effect, doubles the computational cost. At the same time, the fact that mass is lost due to wear needs to be captured by a proper alteration of the proposed formalism. In fact, for closed systems, the conservation of mass is usually neglected because it is satisfied trivially, thus only the conservation of momentum and energy equations are considered. In the case of the wearing tribo-pair, this is clearly not the case. In an effort to reduce computational cost, and at the same account for the mass loss of the deforming members of the tribo-pair, we have explored the idea of reducing the PDE expressing mass conservation in Eq. (6*a*) to a simpler form involving a wear evolution ordinary differential equation (ODE). This was motivated by the fact that many of the low-dimensional wear laws have been expressed in terms of ODEs governing the reduction of wearing zone.

Definition 1. *Let the symbols c_{im}, s_{in}, $w_i(c_{im}; s_{in})$, represent, respectively, the material dependent properties associated with wear, the state variables (such as pressure, velocity, temperature etc.) associated with the multiphysics behavior of the contact pair members, and a function representing how the combination of these material constants and state variables contribute to the ware rate. Also, let i, m, and n represent, respectively, the indexes selecting members from the sets of slider pair, the set of material properties related to wear, and the set of the state variables contributing to wear.*

Under the axiomatic validity of the mass conservation law, the following theorem is proposed:

Theorem 1 (Global Mass Conservation reduces to an ODE). *The global form of the mass conservation law for the control volume of a representative volume element across the interface of a tribo-pair is reducible to a velocity dependent ODE of the form:*

$$\frac{dh_{ie}}{dt} = w_i(c_m; s_n)v, \quad i \in \{s, b\} \tag{7}$$

where h_{ie} represents the wear layer height.

Proof. The global form of the mass conservation law can be expressed by introducing the proper terms (first row) of Table 1, into Eq. (1) to yield

$$\frac{d}{dt}\int_V \rho dV = -\int_S \rho \boldsymbol{v}_b \cdot d\boldsymbol{S} \tag{8}$$

where $\boldsymbol{v}_b$ is the velocity of the wearing mass entering or exiting the control volume of the RVE enclosing the wear domain across the interface.

The control volume of the domain depicted on the right side of Fig. 1 is considered consisting of the sum of the two parallelepiped sub-volumes associated with each of elements of wear-pair such that its size is expressible as of size $dA(h_{se} + h_{be})$, where dA represents the infinitesimal area parallel to the interface and h_{se}, h_{be} are representing the heights of the wear layers for each member of the wear pair, respectively.

Introducing the definition of density $\rho = m/V$ with m and V representing, respectively, the mass and assuming that every control volume that spans the interface does not depend on its neighbors, enables the mass conservation equation to be expressed for each of the partitions (slider and base) of the control volume as follows:

$$\frac{dm_i^{cv}}{dt} = -\rho \dot{h}_{ie} dA_i + \rho v dA_i', \quad i \in \{s, b\} \tag{9}$$

where m_i^{cv} represents the relevant part of the mass of the control volume (denoted by the superscript "cv") and where $\{s, b\}$ represents the set of values for the index i that annotates the mass rates for the case of the slider and base, respectively, and where $\dot{h}_{ie}$, dA_i, v, and dA_i' represent the wear-rate for each element of the pair, the differential area through which this wear is occurring, the velocity of the slider and the differential area through which the worn mass is leaving the control volume, respectively. The negative term signifies the mass entering the control volume while the positive represents the mass leaving the control volume. Since there is no net production of mass in the control volume (i.e. $dm_i^{cv}/dt = 0$), Eq. (9) reduces to

$$\dot{h}_{ie} dA_i = v dA_i', \quad i \in \{s, b\} \tag{10}$$

Rewriting this equation for the wear-rate in terms of wear height h_{ie} per unit time yields

$$\frac{dh_{ie}}{dt} = \frac{dA_i'}{dA_i} v, \quad i \in \{s, b\} \tag{11}$$

The replacements $dA_i' = dz\ dy$ and $dA_i = dz\ dx$ are valid for parallelepiped-shaped representative volume elements (RVEs), where dx and dz represent the infinitesimal lengths along the direction of the motion and the direction normal to the interface, respectively, transform this equation to

$$\frac{dh_{ie}}{dt} = \frac{dy}{dx} v, \quad i \in \{s, b\} \tag{12}$$

The quantity dy/dx represents the evolution of the aspect ratio of the sides of the control volume element involved in the wear processes. In general, this quantity is unknown, and it can be represented as a function $w_i(c_m; s_n)$ that depends on various relevant state variables s_n of the system such as the interfacial pressure p, temperature T, and several material properties c_m such that the friction coefficient μ, the shear strength of the material σ_{ys} that in turn they can also be functions of the state variables as it is known already for the shear strength and the coefficient of friction (COF). Therefore, under the substitution $dy/dx = w_i(c_m; s_n)$, Eq. (12) can now be written as in the expression given by Eq. (7).■

Definition 2. *Let h_i, k_i', p, v, H_i, stand, respectively for the wear height of each of the representative volume element (in the shape of a rectangular parallelepiped) associated with two bodies (*s, b *for slider and base respectively) indexed by* i*, a material dependent constant, the pressure at the interface, the relative velocity between the moving bodies and the hardness of the associated materials. The exponents α_i, β_i, γ_i are also tribo-pair specific properties.*

Corollary 1 (Wear models are representation of wearing volume Mass Conservation). *All ODEs representing the evolution of the wear height h_i of an individual member i of a tribo-pair that have the form*

$$\frac{dh_i}{dt} = k_i' \frac{p^{\alpha_i} v^{\beta_i}}{H_i^{\gamma_i}}, \quad i \in \{s, b\} \tag{13}$$

are actually special cases of the law conservation of mass, under the substitution

$$w_i(k_i', H_i, \alpha_i, \beta_i, \gamma_i; p, v) = k_i' \frac{p^{\alpha_i} v^{(\beta_i - 1)}}{H_i^{\gamma_i}}, \quad i \in \{s, b\} \tag{14}$$

Proof. Introducing Eq. (14) into Eq. (7) trivially produces Eq. (13). ■

It should be underscored here that the wear model given by Eq. (13) is general enough to represent at least thirteen empirically [21–26] and theoretically [27–32] derived one-dimensional wear

models also noted in Ref. [33]. Some of these models have been validated experimentally for specific application regimes. Similarly, the same representation can be applied for most of the 28 wear models described in Ref. [34].

In addition to the wear evolution represented by Eq. (13) additional terms on the right–hand side of this equation can be added to represent additional physics that may or may not depend on pressure, velocity, and material hardness. This will potentially account for the presence of lubricants or erosive thermo-chemical reacting fluids inside the interface introduced either as a consequence of earlier stages of wear or as a result of add-on interfacial fluids, or both. It should also be noted that regardless of how complicated the right–hand side of Eq. (13) turns out to evolve, the wear models represented by this equation is a reduced model in both the syntactic and semantic senses and has the ability to contribute towards the numerical efficiency of the solution associated with the multiphysics system of equations they participate.

Computational Framework

System of Differential Equations Specification. The set of coupled equations that need to be solved for the stated multiphysics wear problem is easily derivable by applying the values in Table 1 into the local form of the generic conservation law given by Eq. (5).

Without loss of generality and after the proper substitutions and simplifications, and assuming slow time–varying applications, the inertial terms and the source terms can be ignored due to the lack of body forces. Therefore, the conservation of momentum can now be expressed as

$$\nabla \cdot \boldsymbol{\sigma} = 0 \tag{15a}$$

$$\boldsymbol{\sigma} = \boldsymbol{C}{:}\boldsymbol{\varepsilon} - \boldsymbol{\beta}(T - T_0) \tag{15b}$$

$$\boldsymbol{\varepsilon} = \frac{1}{2}[\nabla \boldsymbol{u} + (\nabla \boldsymbol{u})^T] \tag{15c}$$

where $\boldsymbol{\sigma}$, $\boldsymbol{\varepsilon}$, $\mathbf{C}$, $\boldsymbol{\beta}$, T, $\boldsymbol{u}$ represent the second-order stress tensor, the second-order strain tensor, the 4th order Hooke's tensor, the 2nd order thermal stress tensor, the temperature, and the displacement vector, respectively. For an isotropic material, this system reduces the Navier–Lame form

$$\nabla\left(\frac{E_i}{2(1+\nu_i)(1-2\nu_i)}\nabla\right)\cdot\boldsymbol{u} + \nabla\cdot\left(\frac{E_i}{2(1+\nu_i)}\nabla\boldsymbol{u}\right) = \frac{E_i\alpha_i}{3(1-2\nu_i)}\nabla T \tag{16}$$

with $i \in \{s, b\}$ and with E_i, ν_i, α_i representing the elastic Young's modulus, Poisson's ratio, and thermal expansion coefficient of the materials, respectively.

Similarly, the proper substitutions of the quantities in Table 1 into the local form of the generic conservation law expressed by Eq. (5) for the case of conservation of energy and after adopting Fourier's law of conduction, produces the well-known form of the heat conduction equation PDEs for each of the members of the pair as follows:

$$\frac{\partial T}{\partial t} = \nabla\cdot\left(\frac{k_i}{\rho_i C_i}\nabla T\right), \quad i \in \{s, b\} \tag{17}$$

where k_i, ρ_i, and C_i represent the heat conductivity, density, and heat capacity of the respective materials, respectively.

Finally, Eqs. (13), (16), and (17) form a coupled system of four PDEs (balance of momentum and energy for two bodies) and two ODEs (wear of two bodies) that fully describe the deformation, heat conduction, and wear physics of the wear-pair problem. The COMSOL multiphysics computational environment [35] was selected for implementing the solution of this system of equations. The discretization of the two PDEs utilized linear hexahedral elements.

A staggered two–step approach was employed as the solution scheme. In the first step, the two PDEs of the momentum and energy conservation and the two ODEs of the wear evolution (or mass conservation) are solved in a tightly coupled bidirectional manner. COMSOL's deformed geometry solution node that expresses an arbitrary–Lagrangian–Eulerian deformation of the mesh in order to represent the wear induced change of the geometry is implemented as the second step. The contact problem for the degrading interface in the structural mechanics context is also solved with the penalty method.

Material Systems Specifications. Two distinct tribo-pairs were selected with the intention of identifying the effects of the presence of a partial glass layer of the base as compared the case when the glass layer is not present.

The reference case was selected to be represented as depicted in Fig. 2 (left). Due to the symmetry across of the $x-y$ plane only half of the system is modeled. The material of the slider was selected to be Aluminum 6061T6 alloy, and the material of the base was selected to be UNS C18100 copper alloy. For the second case, everything is identical with the first (reference system) with the exception that the base contains a thin layer of silica glass extending partially through the thickness of the base and the slider as shown in Fig. 2 (right).

Boundary Conditions Specification. The bottom of the base is considered fixed (i.e., $\boldsymbol{u}|_b = 0$), while a vertical displacement is applied on the top of the slider as a function of time as described in Fig. 3. A reciprocating (sinusoidal) horizontal displacement is also applied on top of the slider; the time evolution of the horizontal displacement and velocity for a frequency $f = 0.5$ Hz are shown in Fig. 4, while the respective horizontal velocity evolution is shown in Fig. 5, respectively. The dashed vertical lines in all of these last three figures represent the times where the spatial distributions of the solution field results are subsequently plotted.

The vertical motion of the slider downward is initiated first from an initial position where its bottom surface is 1 mm away from the top surface of the base. The horizontal sinusoidal motion follows 1 s after the vertical motion has reached its steady-state level. A friction model between the elements of the tribo-pair has been considered to allow for both static and dynamic friction along with a velocity-dependent Stribeck term [36] according to

$$\mu = \mu_{dyn} - (\mu_{stat} - \mu_{dyn})e^{-\alpha_{def}|v|} + a_s|v| \tag{18}$$

where the static, the dynamic, and the Stribeck friction coefficients are set to $\mu_{stat} = 0.3$, $\mu_{dyn} = 0.25$ and $a_s = 0.001$, respectively, for the case of the Aluminum 6061T6—NS C18100 copper pair. The case of the Aluminum 6061T6—Soda lime glass pair is discussed in the "Specification of Wear Models" section.

Thermal insulation boundary conditions have been applied to all boundaries except the interface surfaces for the heat conduction PDE representing the energy conservation. Heat flux boundary conditions have been used for the interface surfaces. The friction generated thermal flux q is evaluated by relation

$$q = \mu p v \tag{19}$$

It should be pointed out that the fluxes applied to each of the members of the wear pair are two complementary partitioning fractions of this flux according to

$$q_s = a\mu p v, \quad q_b = (1-a)pv \tag{20}$$

with the partitioning factor a defined as [37]

$$a = \frac{k_s}{k_s + k_b\sqrt{\dfrac{\kappa_s}{\kappa_s + vL_{sx}}}} \tag{21}$$

where κ_s, L_{sx} represent the heat diffusivity and the length along the motion axis of the slider, respectively.

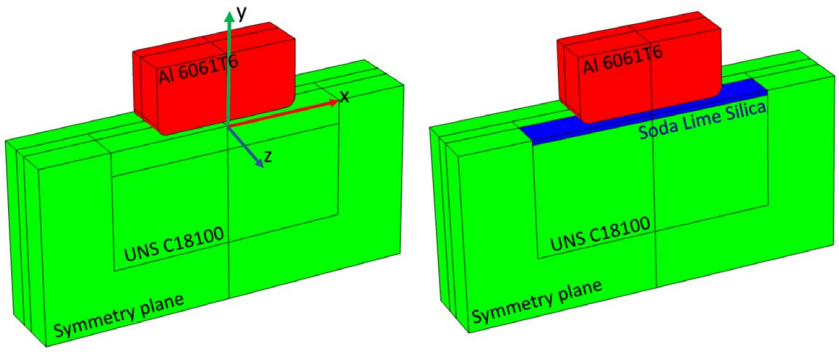

Fig. 2 Computational domains and material specification of reference wear pair (left) and wear pair with glass layer (right)

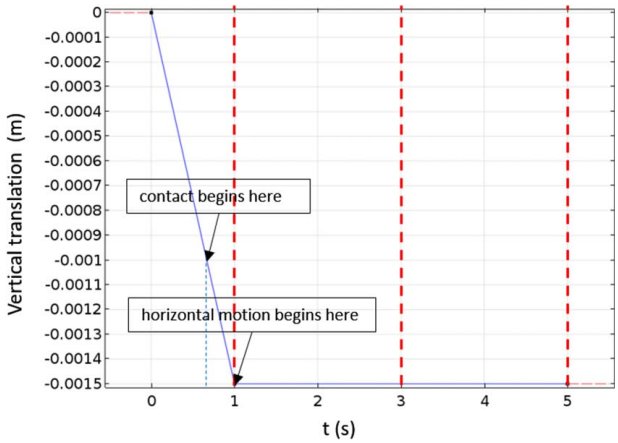

Fig. 3 Vertical displacement specification imposed on the top side of the slider

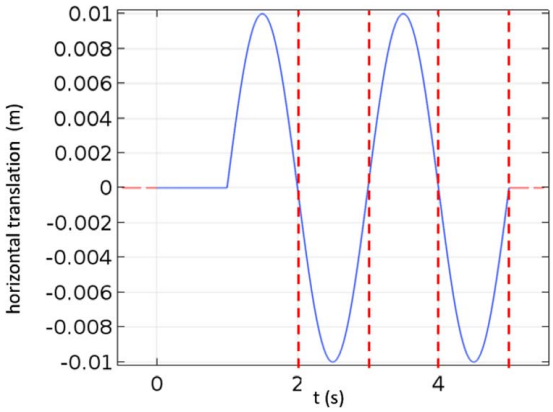

Fig. 4 Horizontal displacement specification imposed on the top side of the slider for the case of $f = 0.5$ Hz

Specification of Wear Models. The evolution of wear was modeled by two instances (one for each member of the wear pair) of Eq. (13) by setting $\alpha_i = \beta_i = \gamma_i = 1$ for $i = \in \{s, b\}$ (Archard equivalent case). However, to enrich the applicability of our framework, the wear laws were further enriched. To account for the temperature dependence of hardness, the relation of hardness with the yield strength as defined in Ref. [38] is considered:

$$H_i = 3Y_i(0.1)^{-n_i}, \quad i = \in \{s, b\} \tag{22}$$

where Y_i, n_i represent the yield strength and hardening exponent of the participating materials. Furthermore, to account for the yield strength reduction as a function of temperature, one of the temperature dependence models of yield strength given by Ref. [39] was adopted in the form

$$Y_i = Y_{ci} - Y_{mi} \tanh\left(\frac{T - T_{ci}}{2\Delta T_{0i}}\right), \quad i = \in \{s, b\} \tag{23}$$

where Y_{ci}, Y_{mi}, T_{ci}, ΔT_{0i} are material dependent constants that can be established by fitting Eq. (23) to experimental data but nevertheless can be assigned physical meaning as described in Ref. [39].

The potential dependence of the wear law from the friction behavior of the system was introduced in a manner that relates the wear coefficient with the friction coefficient according to Ref. [40]

$$k_i' = k_i'' \mu_i^{m_i}, \quad i = \in \{s, b\}, \quad 4 < m_i < 5 \tag{24}$$

with k_i'', m_i representing the friction independent wear coefficient and a material constant considered to have the value $m_i = 4.5$ for the simulations conducted here.

It should be noted that for the case of friction between glass and Al6061T6 we could not find in the literature relevant coefficients for the Eq. (24). For this reason and based on the static friction coefficient between Al and glass being 0.1 (i.e., one-third of the one for the Al6061T6 and UNS C18100 system), we did not alter any of the constants used in Eq. (18) corresponding to the pair of Al6061T6 and UNS C18100. Consequently, the higher friction coefficients used in the simulation will yield a higher and therefore more conservative wear prediction.

Similarly, a temperature degrading yield strength for the glass was not considered in anticipation of temperatures well below melting and in anticipation of the fact that yield degradation in glass is far more insensitive to temperature than it is for the Al 6061T6 and UNS C181000 metal alloys.

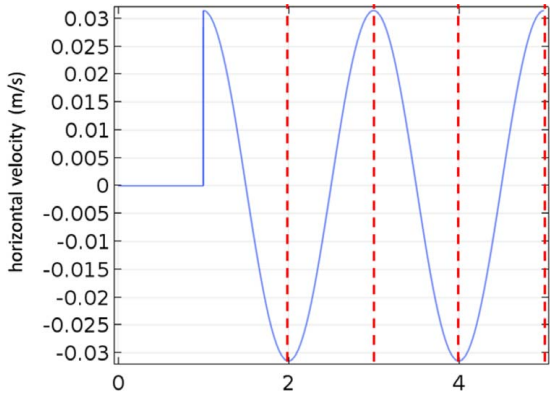

Fig. 5 Horizontal velocity specification imposed on the top side of the slider for the case of $f = 0.5$ Hz

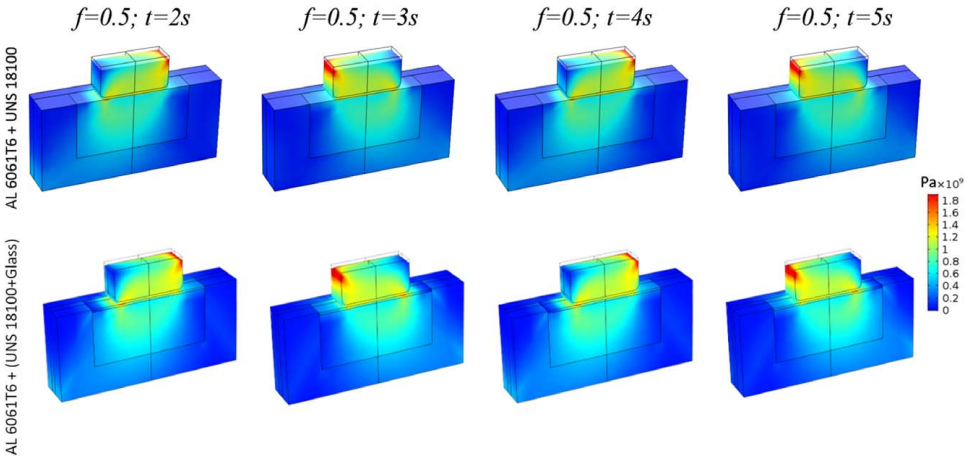

Fig. 6 von Mises stress contours for four time instances associated with the reference tribo-pair (top row) and the glass containing tribo-pair (bottom row) for the case of $f = 0.5$ Hz

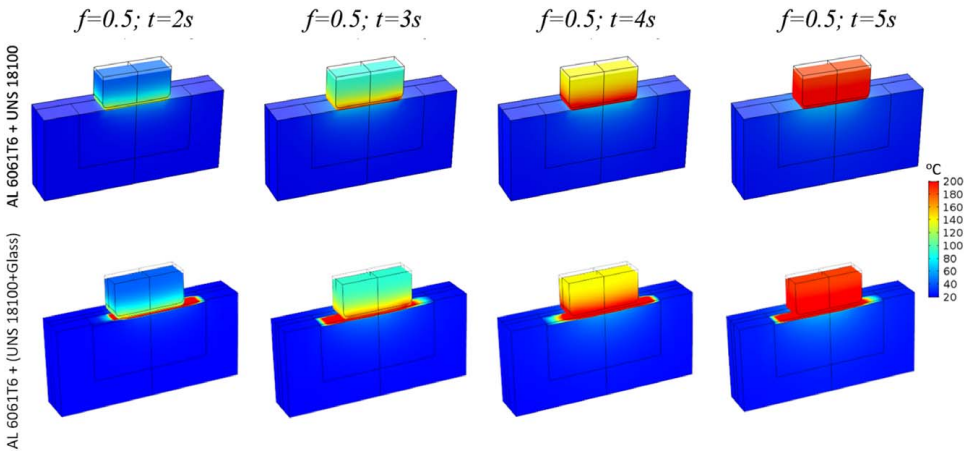

Fig. 7 Temperature contours for four time instances associated with the reference tribo-pair (top row) and the glass containing tribo-pair (bottom row) for the case of $f = 0.5$ Hz

Results of Comparative Numerical Experiments

Application of the developed multiphysics computational framework produced a set of comparative results for various fields associated with the two distinct tribo-pair configurations. Figure 6 shows the contours of von Mises stresses fields developed as a result of the frictional pressure and velocity-dependent heat flux at times $t = 2, 3, 4, 5$ s.

It is worthwhile mentioning that although these results have been plotted at the position where the origin for the motion was initiated, a skewness on the distribution that corresponds to the direction of the velocity vector that activates the interfacial friction that applies shear forces opposing the motion is noted. Furthermore, comparison between the von Mises stress distributions between the two tribo-pairs indicates that the presence of glass in the second one (bottom row) has a very small impact. The only very slight difference appears as faint localizations in the glass layer under the front and rear edges of the slider.

Figure 7 shows the contours of temperature fields developed as a result of the frictional pressure and velocity dependent heat flux at times $t = 2, 3, 4, 5$ s. An obvious first observation is that the temperature field exhibits the cumulative monotonic effect expected from multiple reciprocating cycles that is more pronounced for the case of the slider for both tribo-pairs. Comparison between the two pairs reveals some important differences. The insulative character of glass does not allow the heat generated at the interface to diffuse inside the base substrate and leads to a faster accumulation of heat at the interface that also leads to a quicker temperature rise in the slider.

Similarly, Fig. 8 presents the contours of the spatial distribution of the wear fields on the surface of the slider at times $t = 2, 3, 4, 5$ s. This figure demonstrates the fine structure of the localization of the wear (especially along the edges of the sliders) due to the influence of the thermoelastic response of the system. It also demonstrates the cumulative nature of the wear for the sliders of each pair. Despite the spatio-temporal localization of the slider surface wear fields, careful comparison between the respective wear fields of the sliders associated with each pair appear as slightly increased for the case where glass is present on the base. This is expected due to the interface heat not being able to diffuse inside the base because of the glass layer.

Reciprocally, Fig. 9 presents the contours of the spatial distribution of the wear fields on the surface of the base at times $t = 2, 3, 4, 5$ s. This figure also demonstrates the fine structure of the localization of the wear due to the influence of the thermoelastic response of the system. Despite the spatio-temporal localization of the base surface wear fields, careful comparison between the respective wear fields of the sliders associated with each pair appear as slightly decreased for the case where glass is present on the base.

For a more quantitative comparison and in order to examine the temporal evolution of the wear as a function of frequency, the

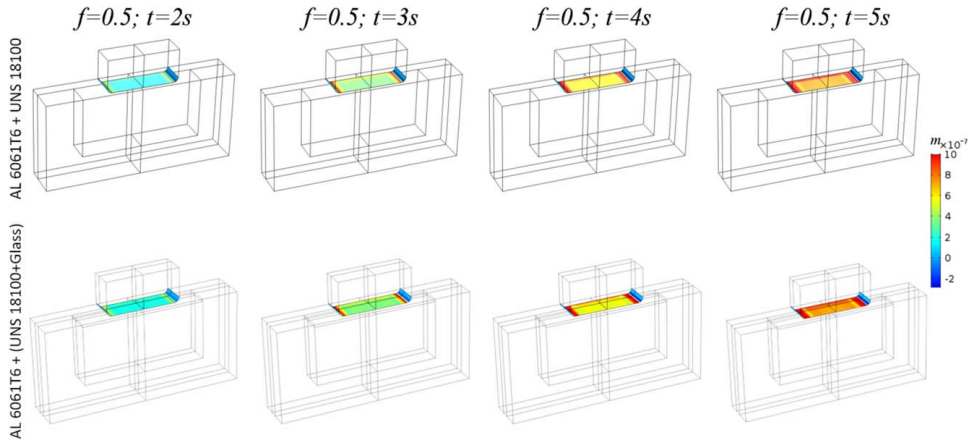

Fig. 8 Contours of slider wear fields for four time instances associated with the reference tribo-pair (top row) and the glass containing tribo-pair (bottom row) for the case of $f = 0.5$ Hz

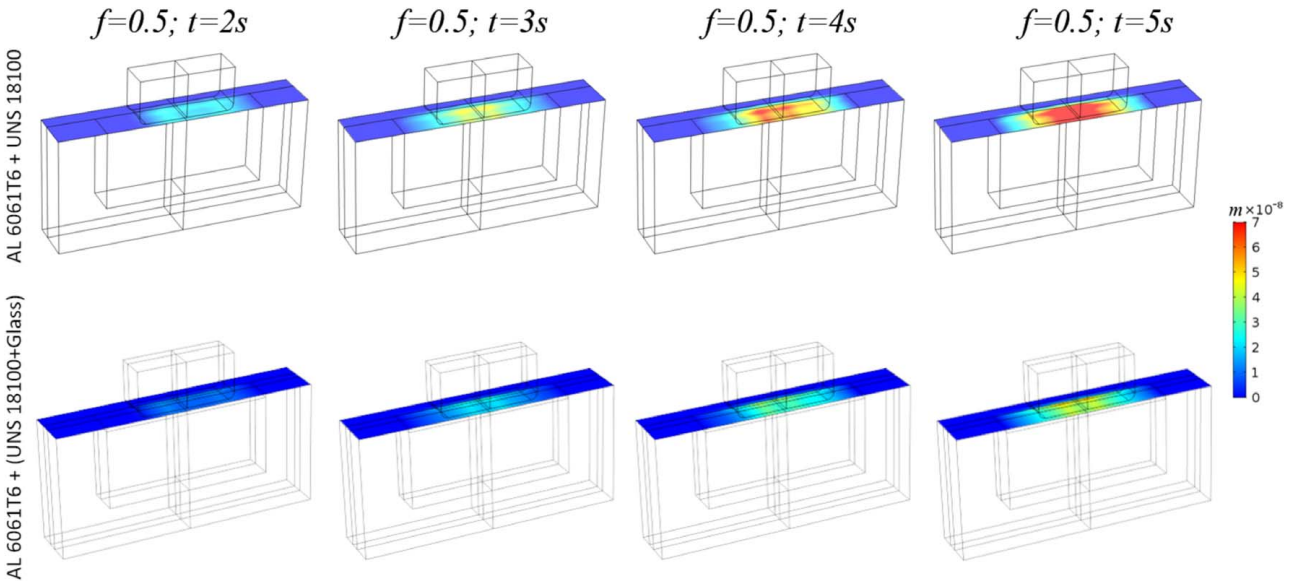

Fig. 9 Contours of base wear fields for four time instances associated with the reference tribo-pair (top row) and the glass containing tribo-pair (bottom row) for the case of $f = 0.5$ Hz

midpoints of the slider and base at the plane of symmetry were selected to plot their time history for the two pairs in Fig. 10 for the cases of $f = 0.3$ Hz, 0.4 Hz, and 0.5 Hz. Clearly, the slider for both pairs shows much higher wear than the respective base and the time evolution is monotonic as expected due to the irreversibility of the wear process. It is also observed that the higher values corresponds to higher frequencies. Another noteworthy observation is the fact that the simulation captures the monotonic nature of wear as well as the variations introduced by the changes in velocity due to its sinusoidal nature. Visual comparison between the wear of the slider at the midpoint between the two tribo-pairs as depicted in Figs. 10(*a*) and 10(*b*), respectively, indicates that there may be no difference between them. Nevertheless, a difference does exist, but it is only of an order less than 1%. Since the same friction coefficients for the two pairs have been used as previously mentioned, the small wear performance differential can be attributed to the effect that temperature has on the rest of the temperature dependent quantities.

It is also observable that the wear at the midpoint of the base for the case of the glass tribo-pair is lower than the respective one for the base of the pair that does not contain glass. For a more detailed comparison, Fig. 11 presents the wear at the midpoint of the bases associated with both pairs. It is evident that for all frequencies, the wear of the base containing the glass is significantly less than that of the pair that does not contain the glass.

Conclusions and Future Plans

An overview of a previously introduced multiphysics framework accounting for the coupling of the thermomechanical interaction of wearing deformable heat conductors in contact in a manner that is aware of the momentum, energy, and mass conservation was outlined in this paper. The framework was applied for an Al 6061T6/UNS C18100 slider/base pair, and an Al 6061T6/UNS C18100 slider/base where the base contains a thin layer of soda lime glass. The slider for both pairs is moving under pressure and under a reciprocating motion governed by a sinusoidal time history.

The proposed framework is capable of computing both the wear of the slider and the base along with the participating state variable fields in a self-consistent manner that obeys the mass, momentum and energy conservation principles.

An important feature of the framework exercised here is the fact that it allows for the implementations of many low order wear models. Another key feature of the present work is that the mass

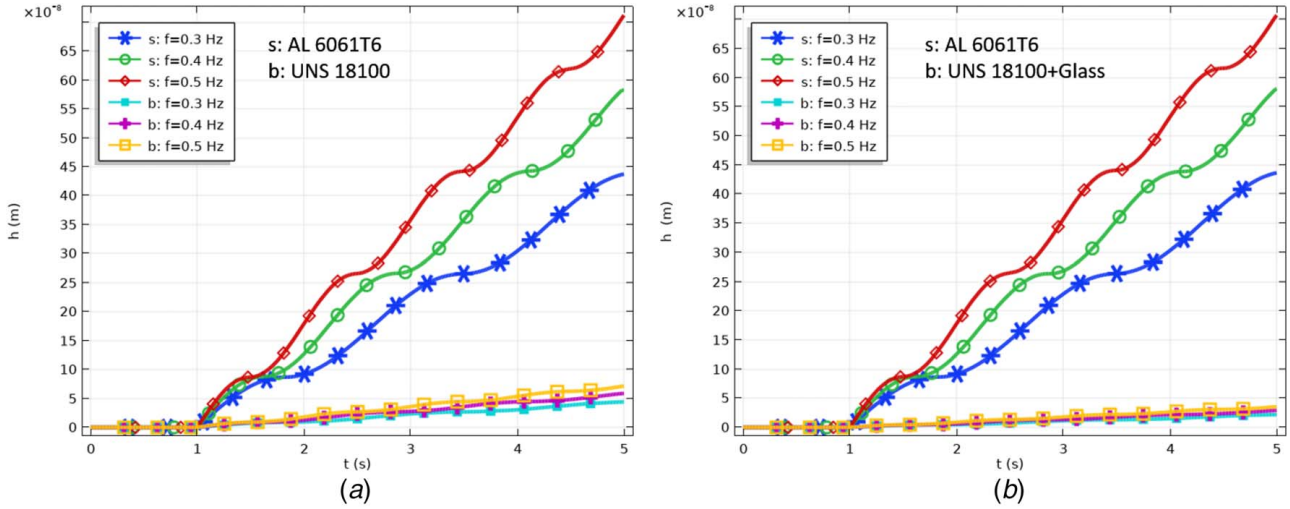

Fig. 10 Time evolution of the wear recession at the midpoints of the slider and the base on the symmetry plane of the two tribo-pairs (no glass (*a*) and with glass (*b*)) for three values of frequency $f = 0.3$ Hz, 0.4 Hz, 0.5 Hz

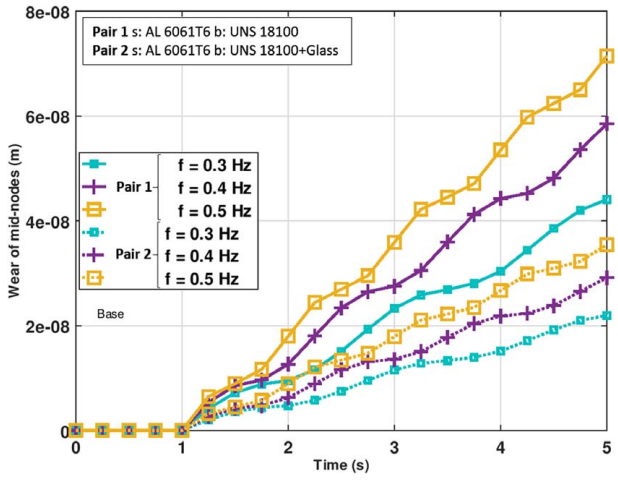

Fig. 11 Time evolution of the wear recession at the midpoints of the base on the symmetry plane of the two tribo-pairs (no glass and with glass) for three values of frequency $f = 0.3$ Hz, 0.4 Hz, 0.5 Hz

conservation representing the wear behavior does not need to be accounted for in the form of PDEs but rather only in the form of ODEs. Consequently, a significant reduction of the computational cost can be realized. A third feature of this framework is that it enables computing wear of both slider and base in a self-consistent manner that accounts for the mutual presence and interaction between them.

Exercising the framework for two tribopairs, one with metal-to-metal and another with metal-to-glass and -metal enabled comparative predictions between the two systems. It was shown that for the case of the pair containing glass on the base, although it leads to increased heat at the interface due the thermal insulation properties of the glass, it still results in lower wear of the base both from qualitative and quantitative perspectives.

Planed future steps include the following: the verification of the framework's functionality for high velocities; its extension to include additional physics such as electromagnetic fields; the characterization of criticality of the influence of participating parameters to wear via a proper sensitivity analysis; and the quantification and propagation of the uncertainty relevant to the variability of the relevant model parameters and their effect on the important quantities of interest. Finally, validation of the predictive capability of the framework will be pursued for various choices of wear physics models.

Acknowledgment

The authors acknowledge support for this work by the Office of Naval Research (ONR) through the Naval Research Laboratory's core funding and through contract N0001418WX01670. The authors also acknowledge the encouragement for pursuing this research by Drs. R. Barsoum of ONR and P. Dudt of the Naval Surface Warfare Center Corderock Division.

References

[1] Põdra, P., and Andersson, S., 1999, "Simulating Sliding Wear With Finite Element Method," Tribol. Int., **32**(2), pp. 71–81.
[2] Po, P., 1999, "Simulating Sliding Wear With Finite Element Method," Tribol. Int., **32**(2), pp. 71–81.
[3] Molinari, J. F., Ortiz, M., Radovitzky, R., and Repetto, E. A., 2001, "Finite-Element Modeling of Dry Sliding Wear in Metals," Eng. Comput., **18**(3/4), pp. 592–609.
[4] Hegadekatte, V., Huber, N., and Kraft, O., 2005, "Finite Element Based Simulation of Dry Sliding Wear," Modell. Simul. Mater. Sci. Eng., **13**(1), p. 57.
[5] Zmitrowicz, A., 2006, "Wear Patterns and Laws of Wear—A Review," J. Theor. Appl. Mech., **44**(2), pp. 219–253.
[6] Martínez, F., Canales, M., Izquierdo, S., Jiménez, M., and Martínez, M., 2012, "Finite Element Implementation and Validation of Wear Modelling in Sliding Polymer-Metal Contacts," Wear, **284–285**, pp. 52–64.
[7] Rezaei, A., Paepegem, W. V., Baets, P. D., Ost, W., and Degrieck, J., 2012, "Adaptive Finite Element Simulation of Wear Evolution in Radial Sliding Bearings," Wear, **296**(1), pp. 660–671.
[8] Woldman, M., Heide, E. V. D., Tinga, T., and Masen, M. A., 2017, "A Finite Element Approach to Modeling Abrasive Wear Modes," Tribol. Trans., **60**(4), pp. 711–718.
[9] Michopoulos, J. G., Iliopoulos, A., and Young, M., 2012, "Towards Static Contact Multiphysics of Rough Surfaces," Proceedings of the ASME 2012 International Design Engineering Technical Conferences and Computers and Information in Engineering Conference. Volume 2: 32nd Computers and Information in Engineering Conference, Parts A and B, Chicago, IL, Aug. 12–15, ASME , pp. 165-176.
[10] Michopoulos, J. G., Young, M., and Iliopoulos, A., 2013, "Multiscale and Multifield Multiphysics of High Current Pulse Static Contact With Rough Surfaces," ASME 2013 International Design Engineering Technical Conferences & Computers and Information in Engineering Conference IDETC/CIE 2013, Portland, OR, Aug. 4–7.
[11] Michopoulos, J., Marcus, Y., and Iliopoulos, A., 2015, "A Multiphysics Theory for the Static Contact of Deformable Conductors With Fractal Rough Surfaces," IEEE Trans. Plasma Sci., **43**(5), pp. 1597–1610.
[12] Michopoulos, J., and Young, M., 2014, "Coupled Electromagnetic and Structural Response for Determining EM Launcher Armature-Rail Interface Mechanical Fields," 5th DoD Innovative Science and Technology Electromagnetic Railgun Workshop, Washington, DC, Oct. 7, ONR.

[13] Michopoulos, J. G., Iliopoulos, A. P., Steuben, J. C., and Birnbaum, A. J., 2018, "On the Multiphysics Modeling of the Sliding Wear Between Deformable Heat Conducting Bodies," Proceedings of the ASME 2018 International Design Engineering Technical Conferences and Computers and Information in Engineering Conference. Volume 1A: 38th Computers and Information in Engineering Conference, Quebec City, Quebec, Canada, Aug. 26–29, p. V01AT02A015.
[14] Michopoulos, J. G., Iliopoulos, A. P., Steuben, J. C., and Birnbaum, A. J., 2019, "On the Effect of Glassy Coatings on the Wear of a Sliding Contact Via Multiphysics Modeling," 39th Computers and Information in Engineering Conference, ASME, Anaheim, CA, Aug. 18–21.
[15] Barsoum, R., and Dudt, P., 2017, "A Proposal for Usage of Glassy Material for Sliding Contact Wear Mitigation," Private Communication.
[16] Panel in Gun Liners, 1954, "Research and Development of Materials for Gun Barrel Intrerior Protection, Materials Advisory Board – National Research Council – National Academy of Sciences, December, Technical Report MAB-86-M.
[17] National Materials Advisory Ad Hoc Committee on Gun Tube Erosion, 1975, "Erosion in Large Gun Barrels," National Materials Advisory Board (NAS-NAE), Technical Report AD-A017-104 and NMAB-321.
[18] Altseimer, J. H., 1977, "The Utilization of Melting Techniques for Borehale Wall Stabilization," Los Alamos Scientific Laboratory of the University of California, American Nuclear Society, Topical Meeting, Energy and Mineral Recovery Research, April 12–14, 1977, Golden, Colorado, April, Technical Report LA-UR-77-840.
[19] Avitzur, B., Beidleman, C. R., Smackey, B. M., and Ache, L. G., 1979, "Potential for Energy Conservation in the Metal Forming Industries," Lehigh University, August, Technical Report COO-4930-1.
[20] Avitzur, B., 1983, *Handbook of Metal-forming Processes* (Ch 9: Tube and Tubular Products), John Wiley and Sons.
[21] Lewis, W. D., 1968, "Fluorocarbon Resin in Piston Rings-New Performance Data for Reciprocating Nonlubrication Air Compressor," Lubrication Eng., **24**, pp. 112–127.
[22] Khrushcov, M. M., and Babichev, M. A., 1970, *Abrasive Wear*, Nauka, Moscow.
[23] Rhee, S. K., 1970, "Wear Equation for Polymers Sliding Against Metal Surfaces," Wear, **16**(6), pp. 431–445.
[24] Lancaster, J. K., 1973, *Tribology Handbook*, Butterworths, London, Ch. Section 4A.
[25] Larsen-Basse, J., 1973, "Wear of Hard Metals in Rock Drilling: A Survey of Literature," Power Metall., **16**(31), pp. 1–32.
[26] Moor, N. B., Walker, B. H., and Appl, F. C., 1978, "A Model of Performance and Life of Diamond Drill Boots," Trans. ASME, Part J: Pressure Vessel Technol., **100**(2), pp. 164–171.
[27] Holm, R., 2000, *Electric Contacts: Theory and Application*, 4th ed., Springer-Verlag, Berlin, Heidelberg, New York.
[28] Archard, J. F., 1951, "Elastic Deformation and the Contact of Surfaces," Nature, **172**(4385), pp. 918–919.
[29] Kragelsky, I. V., 1965, *Friction and Wear*, Butterworths, London.
[30] Rabinowicz, E., 1965, *Friction and Wear of Materials*, John Wiley and Sons. New York.
[31] Rabinowicz, E., 1971, "The Determination of the Compatibility of Metals Through Static Friction Tests," ASLE Trans., **14**(3), pp. 198–205.
[32] Harricks, P. L., 1976, "The Mechanism of Fretting and the Influence of Temperature," Ind. Lubrication Technol., **28**(1), pp. 9–17.
[33] Zhu, D., Martini, A., Wang, W., Hu, Y., Lisowsky, B., and Wang, Q. J., 2007, "Simulation of Sliding Wear in Mixed Lubrication," ASME J. Tribol., **129**(3), p. 544.
[34] Meng, H., and Ludema, K., 1995, "Wear Models and Predictive Equations: Their Form and Content," Wear, **181–183**(Part 2), pp. 443–457.
[35] COMSOL, 2017, Comsol multiphysics.
[36] Woydt, M., and Wäsche, R., 2010, "The History of the Stribeck Curve and Ball Bearing Steels: The Role of Adolf Martens," Wear, **268**(11–12), pp. 1542–1546.
[37] Yuan, F., Liou, N.-S., and Prakash, V., 2009, "High-Speed Frictional Slip At Metal-on-Metal Interfaces," Int. J. Plast., **25**(4), pp. 612–634.
[38] Cahoon, J. R., Broughton, W. H., and Kutzak, A. R., 1971, "The Determination of Yield Strength From Hardness Measurements," Metall. Trans., **2**(7), pp. 1979–1983.
[39] Krasil'nikov, V., Savotchenko, S., and Parkhomenko, A., 2010, "Phenomenological Model of Yield Strength Temperature Dependence for Irradiated Materials," Russ. Metallurgy (Metally), **2010**(4), pp. 292–295.
[40] Challen, J., Kopalinsky, E., and Oxley, P., 1987, "An Asperity Deformation Model for Relating the Coefficients of Friction and Wear in Sliding Metallic Friction," Tribology–Friction, Lubrication and Wear. Fifty Years on., **190**(2), pp. 145–154.